

# MAGNETIC MAPPING OF KILN REMNANTS AT BISTRUP, DENMARK

POUL-ERIK JAKOBSEN and NIELS ABRAHAMSEN

Geological Institute, Laboratory of Geophysics, Aarhus University,  
Finlandsgade 6—8, DK-8200 Aarhus N.

## Locality

Bistrup is situated a few kilometres NNW of Roskilde, Denmark (fig. 1). In the year of 1976 an excavation of the area was carried out by Birgit Als Hansen and Morten Aamann Sørensen, Danish National Museum, Copenhagen (see also Hansen and Sørensen, 1980). The archaeologists uncovered the remnants of five medieval kilns (fig. 2), mainly consisting of floors, remains of the walls, and with debris and recent soil filling the room between the wall remains (see fig. 3).

During the excavation a smaller number of bricks were removed for different kinds of analysis. After finishing the excavation, the area was re-established by putting back the debris and soil to its primary bed between the walls. This means that the situation in 1982, seen from a geophysical prospecting point of view, is very much like the virgin one from before the excavation in 1976. Because of this the results of the magnetic mapping performed in the autumn of 1982 by P.-E. Jakobsen are very much the same as would have been obtained if a survey was carried out before the excavation in 1976.

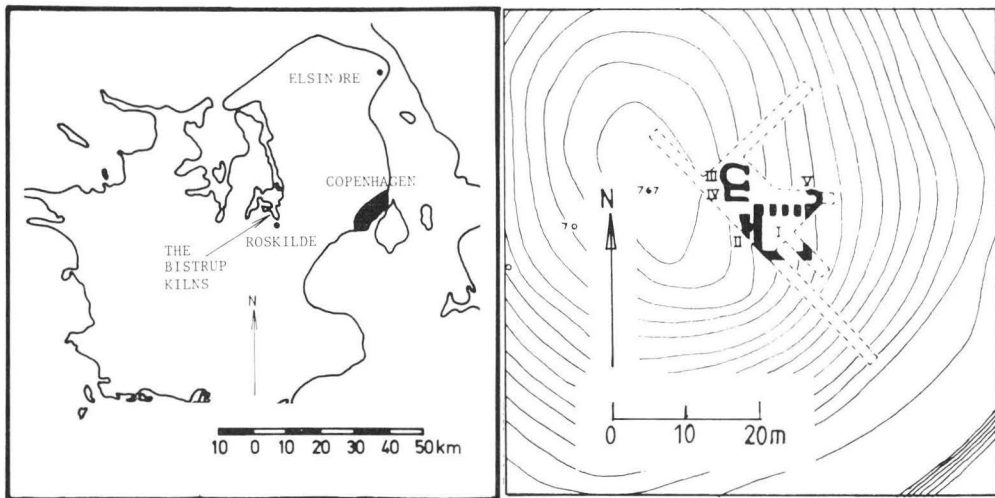


Fig. 1

Fig. 1. Map showing the island of Zealand, Denmark.

Fig. 2

Fig. 2. Plan of the excavation in 1976, equidistance 25 cm. Redrawn from Hansen and Sørensen (1980).



Fig. 3. Remains of kilns I and II (upper right corner) seen from NE. After Hansen and Sørensen (1980).

## Principles and Problems in Magnetic Surveying

### *Area of investigation*

The surveyed area with the kiln remnants was divided into 7 squares, each  $20 \times 20 \text{ m}^2$  (fig. 4) and numbered 1, 2, 3, . . . , 51, 52, 53 and so on to fit into the used EDP-system named the "KORT"-system (Nielsen). Data were sampled for every metre both in the N-S and the E-W direction. The "KORT"-system handles squares with  $21 \times 21 = 441$  data points in each square (whence the  $20 \times 20 \text{ m}^2$ ), and it is possible to work with 50 squares in the N-S and 50 squares in the E-W direction; therefore, the above-mentioned numbering. In the present survey we deal with the squares numbered 2, 3, 52, 101, 102 and 103, so nearly 3100 data were sampled in  $2 \frac{1}{2}$  days of work.

The altitude of measurement was chosen to 1 metre above the ground, partly because the magnetic sources were expected to be of relatively high intensity, and partly in order to smooth the possible geological noise.

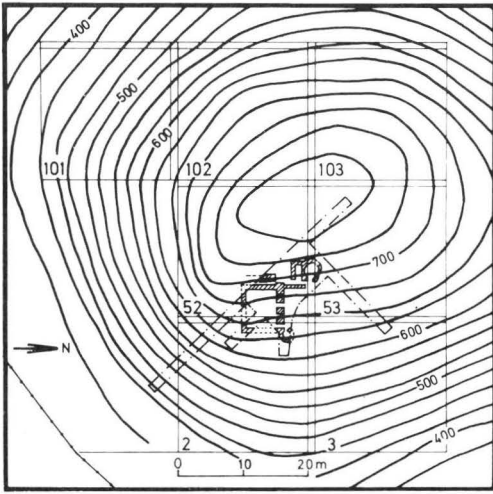


Fig. 4

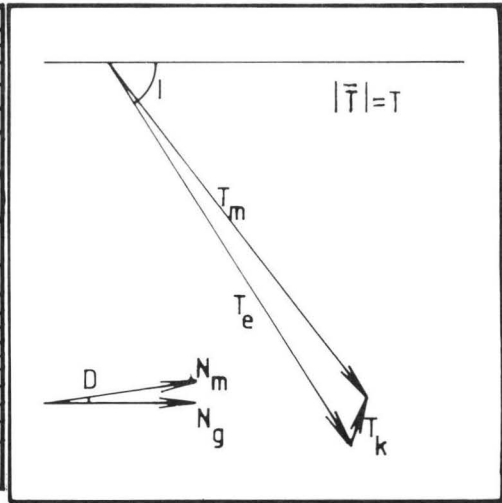


Fig. 5

Fig. 4. The surveyed area with the 7 squares, and the plan of excavation. After Abrahamsen et al. (1984) and Hansen and Sørensen (1980).

Fig. 5. The main features of the magnetic field.

### Magnetic background and surveying principles

At any point on the Earth's surface the magnetic field  $\bar{T}_e$  has a specific magnitude and direction (fig. 5). In Denmark the magnitude is  $\approx 49000$  nT, and the direction is given by the inclination  $I$  and the declination  $D$ ;  $I$  is the angle between the horizontal plane and the field vector, and the present value is about  $70^\circ$ .  $D$  is the angle between magnetic north and geographic north, and the present value is  $1-2^\circ W$ .

The local field  $\bar{T}_k$  from the kilns adds vectorially up to  $\bar{T}_e$ , so  $\bar{T}_m = \bar{T}_e + \bar{T}_k$ . The proton precession magnetometer used detects the magnitude of  $\bar{T}_m = |\bar{T}_m| = T_m$ , which means the total field from the Earth and the kilns. But unfortunately, the magnitude of  $\bar{T}_e$  varies with time. An example is shown in fig. 6, and it is seen that a change in the Earth's magnetic field of 10 nT or even more within a few minutes may occur.

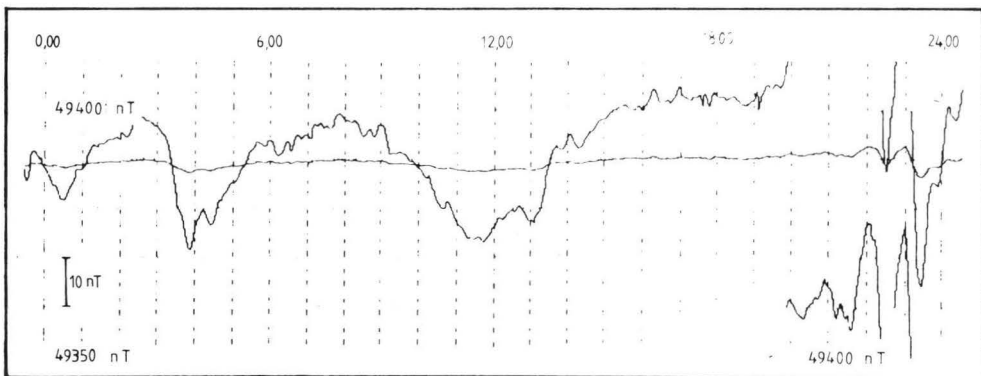


Fig. 6. An example of the variation of the magnetic field. Djursland, Denmark, 01. 11. 83. After Abrahamsen et al. (1984).

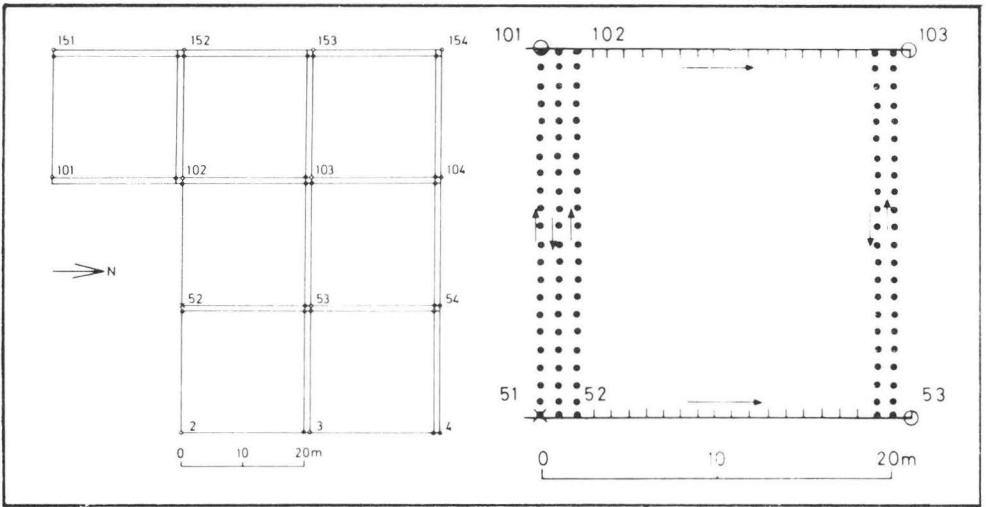


Fig. 7a

Fig. 7b

Fig. 7. a. The 7 squares with the numbering. b. Square number 52 magnified, showing the baseline and the 21 profiles. After Abrahamsen et al., (1984).

Normally, the problem with the time variation is overcome by using two instruments sampling simultaneously.

One instrument is then used as a base station at a fixed point measuring  $T_b = T_e + \Delta T$ . Here  $\Delta T$  is the departure of the measured value  $T_b$  away from a chosen zero point value of  $T_b = T_e$ . The other instrument is moved from point to point in the survey area measuring  $T_f = T_e + \Delta T + T_k$ , where  $T_k$  is the local disturbance, and therefore the disturbance in which we are interested. It is seen that  $T_k$  is determined simply by performing the subtraction  $T_f - T_b$  from the two simultaneous measurements.

Using one instrument only, the procedure is somewhat different. Here we use the linear approximation  $\Delta T = \frac{\partial T_e}{\partial t} \cdot t = k \cdot t$ , which for sufficiently short time intervals  $t$  is a good approximation; so by often returning to a point of known value it is possible to suppress the time variation of the field.

We choose one point to be the base point; in this case the lower left corner of square number 52 (fig. 7a). The field value measured at an arbitrarily selected time  $t = t_0$  is adopted as the true basepoint value. All the following readings are related to this value.

For a constant time interval of 1.0 min. between each reading we now make measurements in all the unknown lower left corners. For each of these measurements we return to the base point 52, so for every 2 minutes we are back at a point of known field value. By thus checking the drift  $\Delta T$ , we are able to determine the field value in all the corner points. (In case of discrepancies the procedure may easily be repeated).

Afterwards the data along all base lines, which means lines between two neighbouring lower left corners, are recorded (fig. 7a + b). Thus the values at the end points are known, and it is now possible to determine the field values in every point on the base lines. The sampling interval may now be as low as 10 sec., and we return to a known point every  $21 \times 10 \text{ sec.} = 210 \text{ sec.} = 3 \frac{1}{2} \text{ min.}$ , as there are 22 sample points in a profile.

Following exactly the same course of action and using the same sample interval, we pick up data along every E-W profile (fig. 7), having 21 profiles in each square. After doing this for all squares it is possible to calculate the field value in every point all over the survey area with an accuracy of a few nT.

#### *Field procedure and data processing*

In practice all the above-mentioned measurements are made continuously, and every reading of 1) the topically magnetic field, 2) number of the profile line, 3) number of the reading, 4) number of Julian Day, and 5) the exact time of reading, is automatically stored in the internal memory of the magnetometer. Back at the laboratory all data are transmitted to the computer centre at the University of Aarhus. Afterwards, sorting of data and calculations are made by the aid of the computer, using programs developed by P.-E. Jakobsen.

Finally, the corrected data are read out on to a file, which can be read by the previously mentioned KORT-system. Using this, we end up with a contour map like the one shown in fig. 8.

#### **Interpretation and a Little Further Background**

What does this magnetic anomaly map tell us? It is rather simple to point out the anomalous area, where we see a nearly circular and a somewhat rectangular anomaly. This means that we are able to point out two objects, which might be examined. Further, and also very important, we may conclude that these are the only objects of archaeo-magnetic relevance within the surveyed area.

In figure 9 we take a closer look at the anomalies with the plan of excavation superimposed. We see a quite good, but not perfect coincidence between the anomaly and

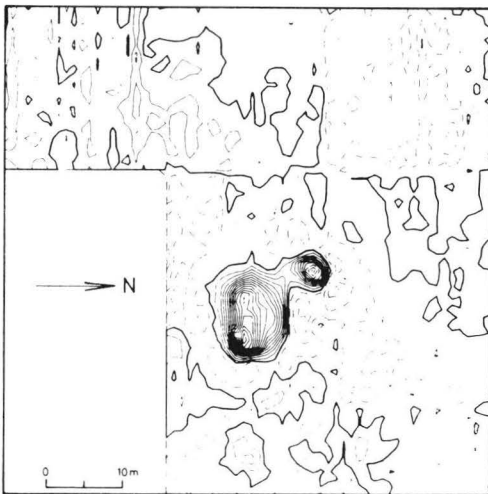


Fig. 8

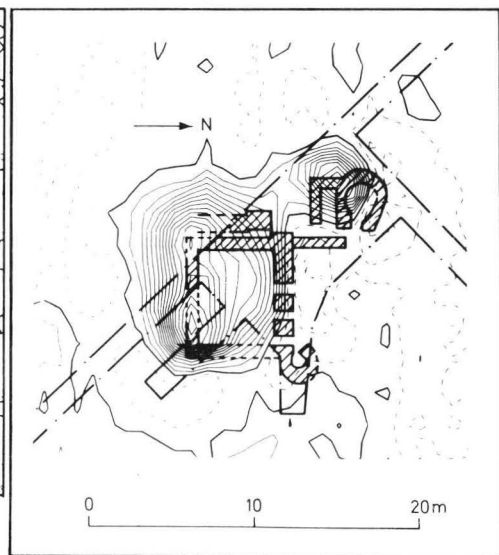


Fig. 9

Fig. 8. Contour map of the surveyed area, equidistance 10 nT. After Abrahamsen et al. (1984).

Fig. 9. A magnified picture of the anomalies with the plan of excavation superimposed, equidistance 10 nT. After Abrahamsen et al., (1984) and Hansen and Sørensen (1980).

the plan of excavation. But is a perfect coincidence to be expected? The answer is negative!

To understand why, we may increase our magnetic knowledge, and take further magnetic information into account. First we may distinguish between induced and remanent magnetization. The former is only existing if we have an external magnetizing field, which we certainly have because of the geomagnetic field, formerly named  $\bar{T}_e$ . Further, the angles I and D for this kind of magnetization are exactly the same as those of the *recent* magnetizing field. Then  $I_{ind} = 70^\circ$ ,  $D_{ind} = 1-2^\circ W$ .

The remanent magnetization can, however, be present in the material even in the absence of an external field, and the direction of the remanent magnetization is given by the direction of the field at the time when the material was last cooling down from a certain high temperature, known as the Curie temperature. Therefore, the remanent magnetization has the direction of the ancient magnetic field. (The long-term variation of I and D is named the geomagnetic secular variation).

These ancient values for I and D are known from the former investigations (Abrahamsen et al., 1982) as follows:

$$\begin{array}{llll} I_I = 74.5^\circ & I_{II} = 68.1^\circ & I_{III} = 66.6^\circ & I_{IV} = 85.6^\circ \\ D_I = 12.8^\circ E & D_{II} = 8.8^\circ E & D_{III} = 8.3^\circ E & D_{IV} = 11.3^\circ W \end{array}$$

(It should be mentioned that  $I_{IV}$  is unusually high, which may be due to influence by the local field from the neighbouring kilns).

The influence of the inclination on the positioning of the anomaly is demonstrated in fig. 10 a + b, and the interesting feature is the slight southward displacement of the maximum. This is valid for  $I \approx 70^\circ$ . For increasing I-values, the displacement decreases, and for  $I = 90^\circ$ , no such displacement is seen.

Piecing together the above-mentioned relations we see a very good agreement between theory and the results of the actual survey.

The role of the declination is shown in fig. 10 c; an *eastward declination* of the remanent magnetization of the structure causes a *westward displacement* of the centre of the magnetic anomaly on the northern hemisphere, and vice versa.

The anomalies from kilns I and II actually show a westward displacement in agreement with the declination of the remanent magnetization, but not with the induced magnetization. This just tells us that the remanent magnetization must be of much greater numerical values than the induced one. A fact which is supported by the value of Königsberger's ratio,  $Q_N = \frac{J_{rem}}{J_{induc}}$ , which in the case of kilns I and II is  $Q_I = 52.4$  and  $Q_{II} = 24.1$ , respectively (Abrahamsen et al., 1982).

Looking at the declination values for the present induced magnetization and for the remanent magnetization of kilns III and IV we would not expect any significant E-W displacement. But we do see a westward displacement, in agreement with the declination value of kiln III, so it seems to be the remanent magnetization of kiln III which mainly determines the orientation of the anomaly from kiln III and IV. The Q-values for kiln III and IV again support the fact that the anomaly features are controlled by the remanent magnetization as  $Q_{III} = 34.3$  and  $Q_{IV} = 30.5$ , respectively (Abrahamsen et al., 1982). The reason why the westerly declination of kiln IV is obscured may be the ratio of the magnitude of the remanent magnetization of kiln III to that of kiln IV. Using the data from (Abrahamsen et al., 1982) we get  $J_{r,III}/J_{r,IV} = 6.0/1.8 \approx 3.3$ .

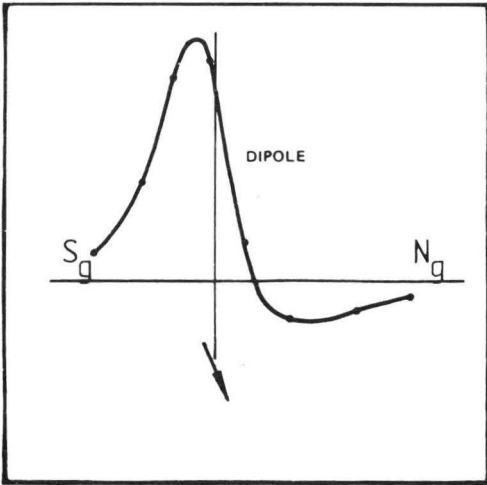


Fig. 10a

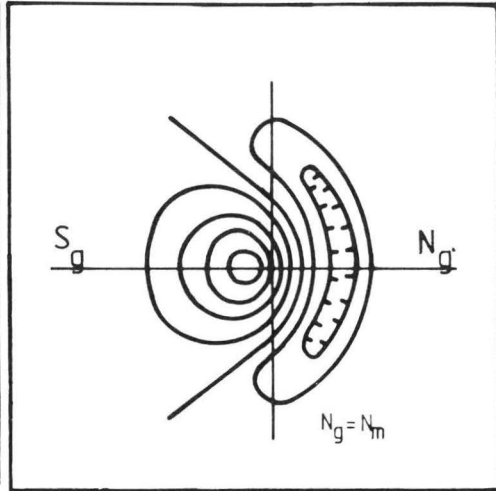


Fig. 10b

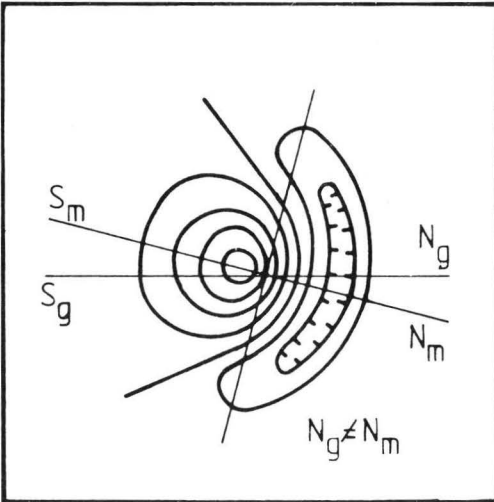


Fig. 10c

Fig. 10. a. The principal profile over a dipping dipole, the effect of  $I$ . Here  $I = 70^\circ$ . b. The contour map of the dipping dipole. c. The effect of  $D$  being different from  $0^\circ$ .  $N_g$  = Geographic North,  $S_g$  = Geographic South,  $N_m$  = Magnetic North,  $S_m$  = Magnetic South. Redrawn from Breiner (1973).

## Conclusion

From what we have seen we may conclude that with the magnetic surveying method we have a rather exact and fairly quick way of pinpointing certain archaeological objects.

In the case of fired materials it may be an advantage if the age is known, because, in this case the knowledge of the variation of  $I$  and  $D$  of the ancient field may improve the interpretation of the anomalies, although a specific, magnetic modelling is seldom justified.

At last it should be mentioned that a great variety of archaeological objects and structures exist, exhibiting a sufficiently strong magnetization which may be sufficiently different from the geological background noise to make them detectable in a magnetic survey like the one presented here (Abrahamsen et al., 1984; Aitken, 1974; Breiner, 1973).

## REFERENCES

- Abrahamsen, N., Hansen, B. Als and Sørensen, M. A., 1982. Palaeomagnetic investigations of four medieval kilns from Bistrup near Roskilde, Denmark. *PACT* 7, 153—167.
- Abrahamsen, N., Jakobsen, P.-E. and Voss, O., 1984. Archaeomagnetic Surveying. In Möller, J. T. and Jörgensen, M. S. (eds): *Arkeologi og geofysiske sporingsmetoder*, 109—144. Working Papers, 14, Danish National Museum, Copenhagen. English summaries.
- Aitken, M., 1974. *Physics and Archaeology*. 271 pp. Oxford University Press.
- Breiner, S., 1973. *Applications Manual for Portable Magnetometers*. 58 pp. Geometrics.
- Hansen, B. Als and Sørensen, M. A., 1980. The Bistrup Tilework. *Hikuin* 6, 221—264. Prehistoric Museum Moesgaard, Aarhus.
- Nielsen, P. H. The Program Package “KORT”-system. Laboratory of Geophysics, Aarhus. Unpublished.